# Recent progress in EDF calculations for heavy nuclei

Michael Bender

Institut de Physique des 2 Infinis de Lyon
CNRS/IN2P3 & Université de Lyon & Université Lyon 1
F–69622 Villeurbanne, France

Workshop on Laser spectroscopy as a tool for nuclear theories

ESNT Saclay, 7–11 October 2019

Quote (falsely) attributed to A. Einstein "Only two things are infinite, the universe and human stupidity, and I'm not sure about the former."

- Calculations presented in what follows were made in a Cartesian 3d coordinate-space code using a "Lagrange-mesh representation" (a special case of discrete variable representation).
- The code allows for breaking time-reversal and/or parity and/or signature, can handle blocked multi-quasiparticle states and constraints on the shape of the density and on angular momentum.
- The latter features can be put to good use for studying spectroscopic properties of heavy nuclei.

Baye, Heenen, JPA19 (1986) 2041

Bonche, Flocard, Heenen, Krieger, Weiss, NPA 443 (1985) 39

Bonche, Flocard, Heenen, CPC171 (2005) 49

Ryssens, thesis, UL Bruxelles (2016)

Ryssens, Hellemans, Bender, Heenen, CPC 187 (2015) 175

Ryssens, Heenen, Bender, PRC 92 (2015) 064318

Ryssens, Bender, Heenen, EPJA 55 (2019) 93

# Relevance of surface tension

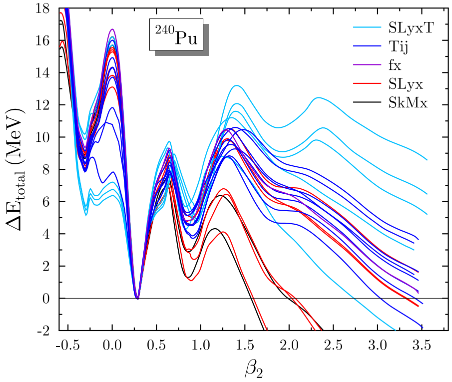


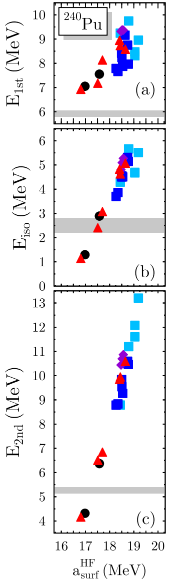


Data:

- inner barrier: 5.95 / 5.8 / 6.1 / 6.05 MeV (depending on source)
- isomer: $2.4 \pm 0.3$ / $\approx 2.8$ / $2.25 \pm 0.20$ MeV (depending on source)
- outer barrier: $\approx 5.4$ / 5.3 / 5.2 / 5.15 MeV (depending on source)

Only few parameterizations describe data reasonably well (SkM*, SLy6, UNEDF2). Fewer underestimate data (SkM & SLy4d), most overestimate it.

Jodon, Bennaceur, Meyer, Bender, PRC94 (2016) 024355

Deformation energy is correlated to the surface energy coefficient

$$E_{\mathrm{LDM}}(N,Z) = (a_{\mathrm{vol}} + a_{\mathrm{sym}}\, I^2)\, A + (a_{\mathrm{surf}} + a_{\mathrm{ssym}}\, I^2)\, A^{2/3} + \frac{3\,e^2}{5\,r_0}\,\frac{Z^2}{A^{1/3}} - \frac{3\,e^2}{4\,r_0}\left(\frac{3}{2\pi}\right)^{2/3}\frac{Z^{4/3}}{A^{1/3}}$$

- Values can be extracted from calculations of the model system of semi-infinite nuclear matter.
- Values are *model-dependent*, i.e. the value for a given parameterization can systematically differ by up to 1.5 MeV depending on calculating it in Hartree-Fock (HF), Extended Thomas-Fermi (ETF), or Modified Thomas-Fermi (MTF).
- Values for Skyrme EDFs cover a wide range of values.

Jodon, Bennaceur, Meyer, Bender, PRC94 (2016) 024355

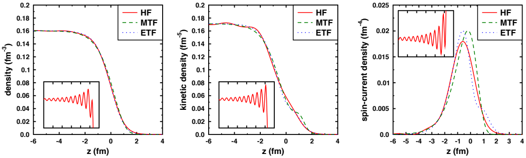


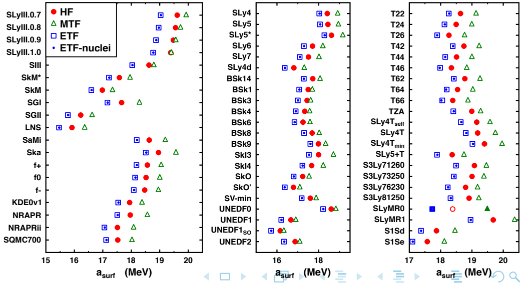

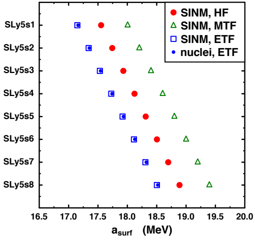


Jodon, Bennaceur, Meyer, Bender, PRC94 (2016) 024355

- systematically varied $a_{surf}$
- Constraint that there are no unphysical finite-size instabilities in any spin-isospin channel

$\Rightarrow$ The SLy5sX can be used without ambiguities in time-reversal breaking calculations (odd nuclei, ...)

- All terms in the EDF (except Coulomb and pairing) contribute to $a_{surf}$.
- $a_{surf}$ cannot be adjusted completely independently from the bulk energy and shell structure.

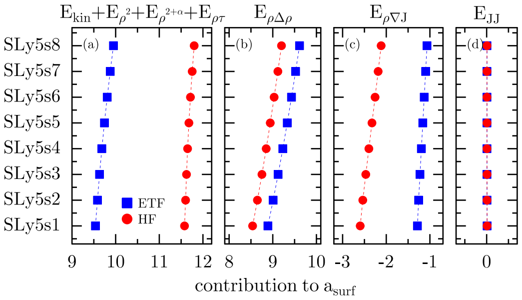


Jodon, Bennaceur, Meyer, Bender, PRC94 (2016) 024355

# Fission barriers: Examples

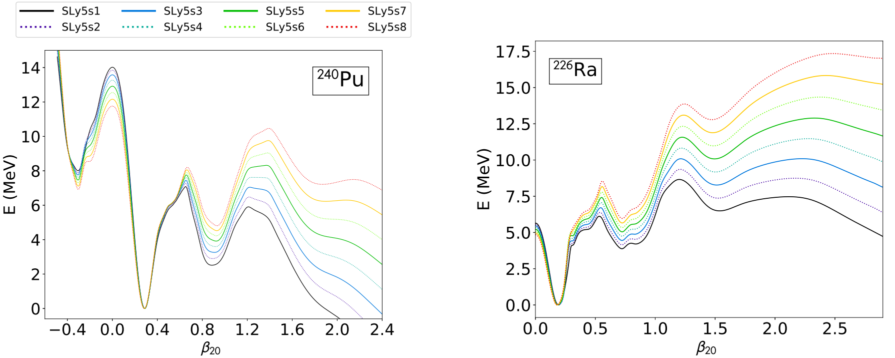


Ryssens, Bender, Bennaceur, Heenen, Meyer, PRC 99 (2019) 044315

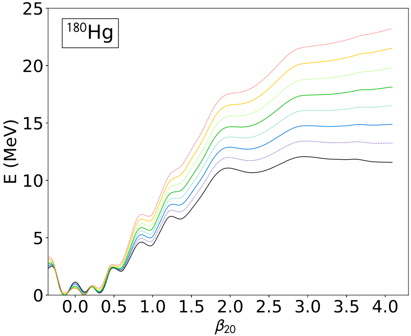


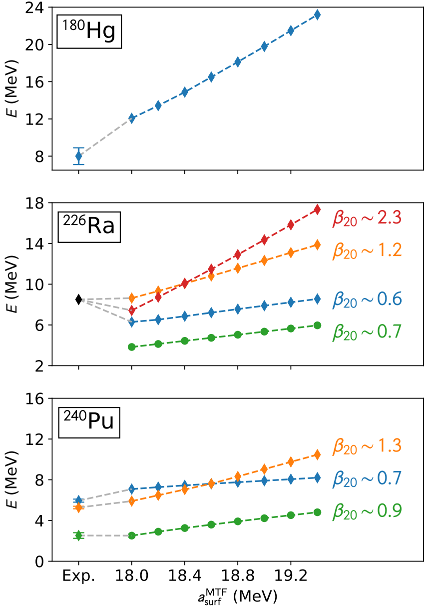


- The larger the deformation of the saddle point, the larger the impact of $a_{\mathrm{surf}}$ on the barrier height.
- Differences at small deformation of $^{180}$Hg are caused by small differences in shell structure. Will be relevant for isotopic shifts of charge radii

Ryssens, Bender, Bennaceur, Heenen, Meyer, PRC 99 (2019) 044315

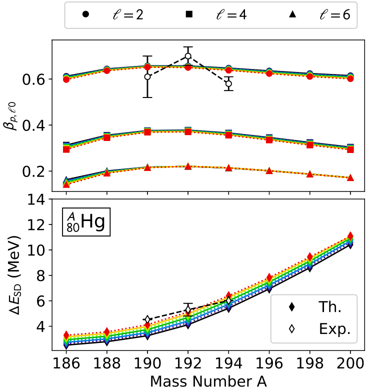


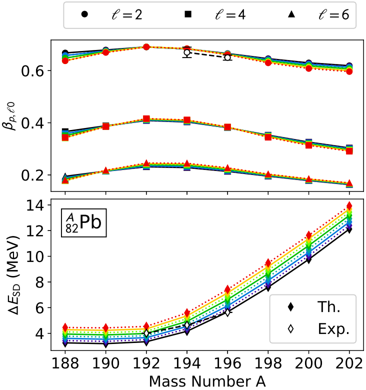


- While the fission barrier of $^{180}$Hg is still too high with SLy5s1, superdeformed minima in nearby Hg and Pb isotopes are too low.
- $\Rightarrow$ problem with shell effects?

Ryssens, Bender, Bennaceur, Heenen, Meyer, PRC 99 (2019) 044315

# Intermission: A word of warning

- Pushing the adjustment of properties of (spherical) doubly-magic nuclei "too far" might spoil properties of other nuclei.
- Example: series of SAMi parameterizations.

- Pushing the adjustment of properties of (spherical) doubly-magic nuclei "too far" might spoil properties of other nuclei.
- Example: series of SAMi parameterizations.

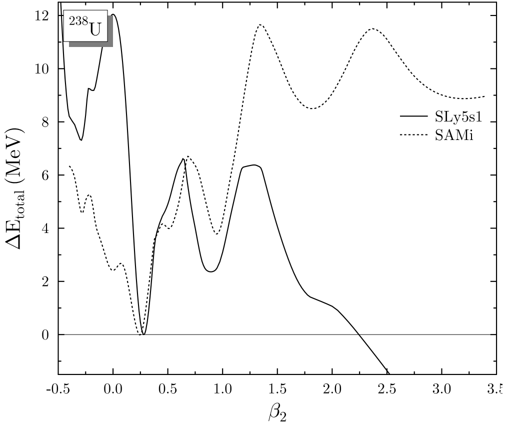


Bender, Meyer, Ryssens, unpublished

- Pushing the adjustment of properties of (spherical) doubly-magic nuclei "too far" might spoil properties of other nuclei.
- Example: series of SAMi parameterizations.

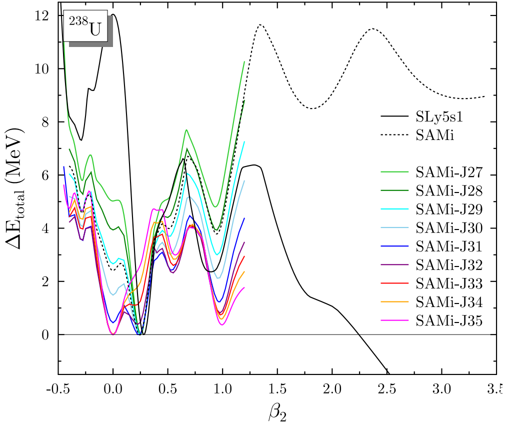


Bender, Meyer, Ryssens, unpublished

- Going from SLy5s8 to SLy5s1, the relative energy of the coexisting minima changes.
- Changing the pairing strength has a similar effect on the relative energy between minima (calculations by Pastore & Dobaczewski).

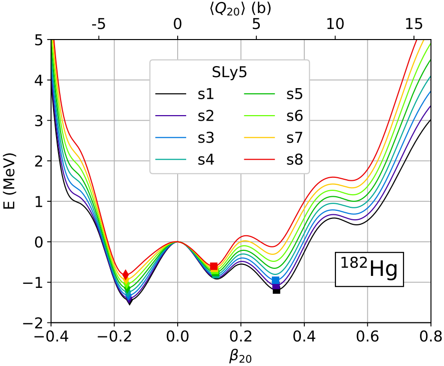


Ryssens, Bender, Heenen (unpublished)

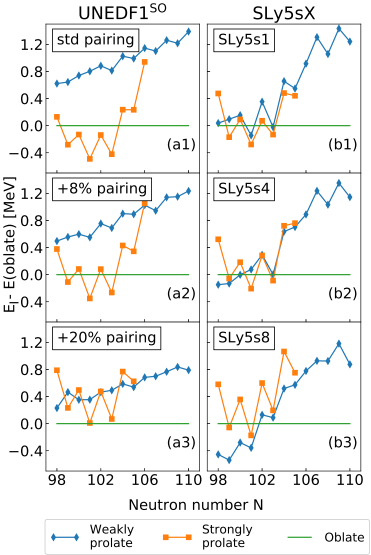


Sels et al, PRC99 (2018) 044306.

- Odd-even staggering of Hg isotopes results from a "happy accident" (JD) in the relative energy between coexisting states, which can be fine-tuned through many details of the EDF.

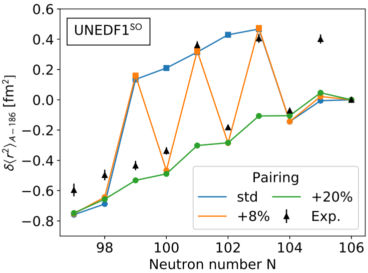


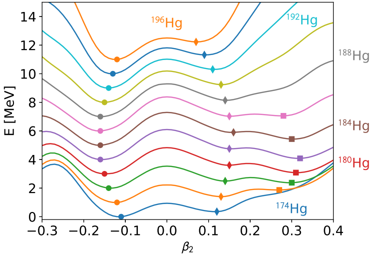


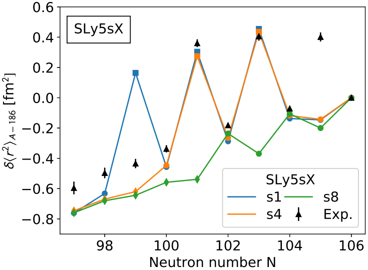


Sels et al, PRC99 (2018) 044306.

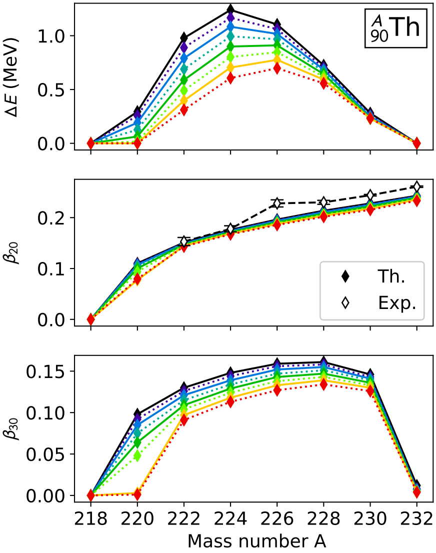


⇐ SLy5s1 (black) to SLy5S8 (red)

⇓ deformation energy of $^{222}$Th with SLy5s1

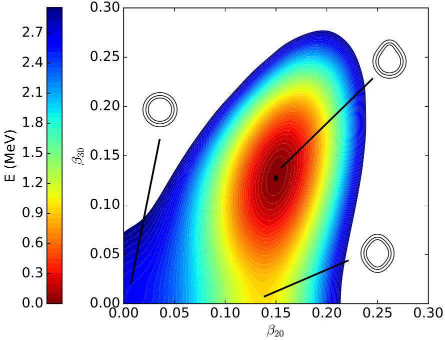


Ryssens, Bender, Bennaceur, Heenen, Meyer, PRC 99 (2019) 044315

deformation energy of $^{222}$Th as a function of $\beta_{30}$ and (cranked) angular momentum ***I*** (see legend) for SLy5s1

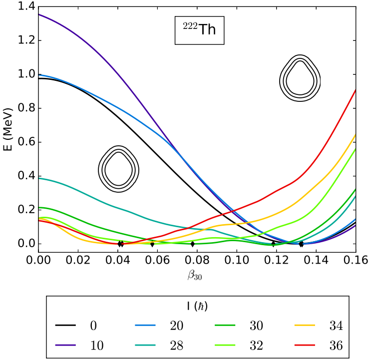


Ryssens, Bender, Heenen, in preparation

rotational band of $^{222}$Th with SLy5s1

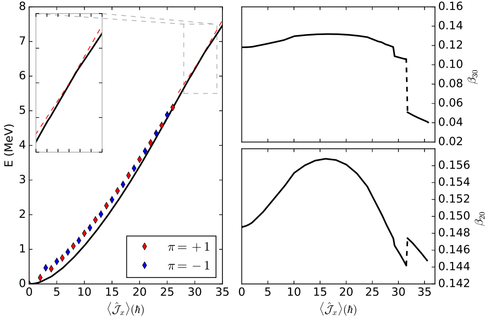


Ryssens, Bender, Heenen, Acta Phys. Pol. B49 (2018) 339.

symmetry-dependence of the spin density of the calculated ground state of $^{223}$Th (arrows) calculated with SLy5s1. Contours indicate the shape of the mass density.
Left: conserved signature, net spin is aligned with symmetry axis of the density.
Right: non-conserved signature, net spin is perpendicular to the symmetry axis of the density.

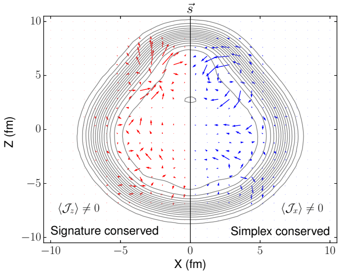


Potentially impacts magnetic moments.

Ryssens, Bender, Heenen, in preparation

enhancement of isotopic shifts

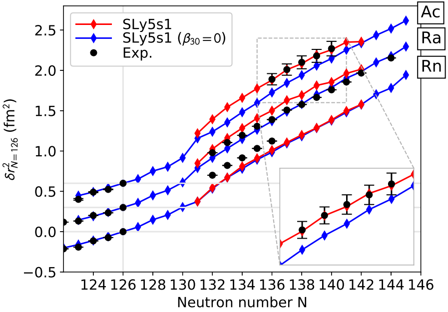


inverted staggering of octupole-deformed Ra

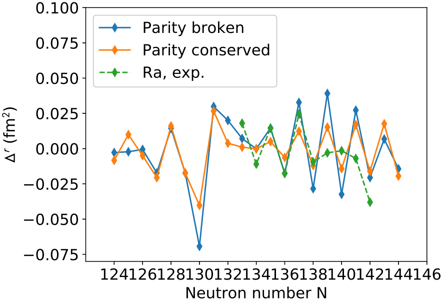


Red: Symmetry-unrestricted calculation (many $N > 130$ isotopes are octupole-deformed)

Blue: Calculation constrained to $\beta_{30} = 0$

Offset from experiment might be related to incorrect description of the $N = 126$ isotope in these chains.

Blue: Symmetry-unrestricted calculation

Orange: Calculation constrained to $\beta_{30} = 0$

The state leading to the lowest binding energy is blocked in the odd nuclei.

Bender & Ryssens, unpublished

- Static octupole deformation can be found up to U isotopes.
- Some nuclides with higher Z remain very soft against octupole deformation.

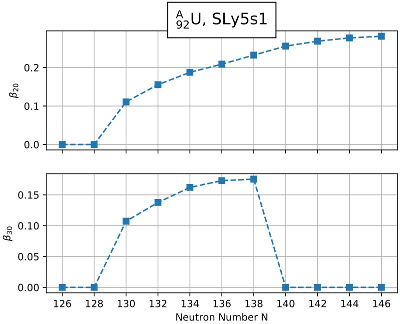


Ryssens & Bender, unpublished

- breaking of time-reversal symmetry for odd (and odd-odd) nuclei
- fully self-consistent blocking in HFB
- SLy5s1 + surface pairing functional

$$E_{\text{pair}}^{\text{ULB}} = \int d^3r \sum_q \tilde{\rho}_q^*(\mathbf{r})\, \tilde{\rho}_q(\mathbf{r}) \left[ A_q^{\tilde{\rho}\tilde{\rho}} + B_q^{\tilde{\rho}\tilde{\rho}\rho} \frac{\rho_0(\mathbf{r})}{\rho_{\text{sat}}} \right]$$

For $V_n = V_p$ and $\alpha_n = \alpha_p$, this form of pairing EDF can be obtained as particle-particle part of the HFB expectation value from a two-body $T = 1$, $S = 0$ contact pairing interaction

$$\begin{aligned} v_{\text{pair}}(\mathbf{r}_1, \mathbf{r}_2, \mathbf{r}'_1, \mathbf{r}'_2) &= \hat{\Pi}_{S=0}\, V_0 \left[ 1 - \alpha \frac{\rho_0(\mathbf{r})}{\rho_{\text{sat}}} \right] \delta_{\mathbf{r}_1,\mathbf{r}_2}\, \delta_{\mathbf{r}_1,\mathbf{r}'_1}\, \delta_{\mathbf{r}_2,\mathbf{r}'_2} \\ &= \tfrac{1}{2} \left( 1 - \hat{P}_\sigma \right) V_0 \left[ 1 - \alpha \frac{\rho_0(\mathbf{r})}{\rho_{\text{sat}}} \right] \delta_{\mathbf{r}_1,\mathbf{r}_2}\, \delta_{\mathbf{r}_1,\mathbf{r}'_1}\, \delta_{\mathbf{r}_2,\mathbf{r}'_2} \end{aligned}$$

- Contribution to single-particle potential

$$U_{\text{pair},q}(\mathbf{r}) \equiv \frac{\delta E_{\text{pair}}}{\delta \rho_q(\mathbf{r})} = \sum_{q'} \tilde{\rho}_{q'}^*(\mathbf{r})\, \tilde{\rho}_{q'}(\mathbf{r})\, B_{q'}^{\tilde{\rho}\tilde{\rho}\rho} \frac{\gamma_{q'}\, \rho_0^{\gamma_{q'}-1}(\mathbf{r})}{\rho_{\text{sat}}^{\gamma_{q'}}}$$

- Fayans pairing energy density functional has an quadrilinear gradient term

$$E_{\text{pair}}^{\text{Fy}} = \int d^3r \sum_q \tilde{\rho}_q^*(\mathbf{r})\,\tilde{\rho}_q(\mathbf{r}) \left\{ A_q^{\tilde{\rho}\tilde{\rho}} + B_q^{\tilde{\rho}\tilde{\rho}\rho} \left[\frac{\rho_0(\mathbf{r})}{\rho_{\text{sat}}}\right]^{\gamma_q} + C_q^{\tilde{\rho}\tilde{\rho}\nabla\rho\nabla\rho} \left[\boldsymbol{\nabla}\rho_0(\mathbf{r})\right]\cdot\left[\boldsymbol{\nabla}\rho_0(\mathbf{r})\right] \right\}$$

which corresponds to a two-body pairing force of the form

$$v_{\text{pair}}(\mathbf{r}_1,\mathbf{r}_2,\mathbf{r}'_1,\mathbf{r}'_2) = \hat{\Pi}_{S=0}\,V_0 \left[1+\alpha\left(\frac{\rho_0(\mathbf{r})}{\rho_{\text{sat}}}\right)^{\gamma} + \beta\left[\boldsymbol{\nabla}\rho_0(\mathbf{r})\right]\cdot\left[\boldsymbol{\nabla}\rho_0(\mathbf{r})\right]\right] \delta_{\mathbf{r}_1,\mathbf{r}_2}\,\delta_{\mathbf{r}_1,\mathbf{r}'_1}\,\delta_{\mathbf{r}_2,\mathbf{r}'_2}$$

- Fayans pairing energy density functional has an quadrilinear gradient term

$$E^{\text{Fy}}_{\text{pair}} = \int d^3r \sum_q \tilde{\rho}^*_q(\mathbf{r})\, \tilde{\rho}_q(\mathbf{r}) \left\{ A^{\tilde{\rho}\tilde{\rho}}_q + B^{\tilde{\rho}\tilde{\rho}\rho}_q \left[\frac{\rho_0(\mathbf{r})}{\rho_{\text{sat}}}\right]^{\gamma_q} + C^{\tilde{\rho}\tilde{\rho}\nabla\rho\nabla\rho}_q \left[\boldsymbol{\nabla}\rho_0(\mathbf{r})\right]\cdot\left[\boldsymbol{\nabla}\rho_0(\mathbf{r})\right] \right\}$$

which corresponds to a two-body pairing force of the form

$$v_{\text{pair}}(\mathbf{r}_1,\mathbf{r}_2,\mathbf{r}'_1,\mathbf{r}'_2) = \hat{\Pi}_{S=0}\, V_0 \left[1+\alpha\left(\frac{\rho_0(\mathbf{r})}{\rho_{\text{sat}}}\right)^{\gamma} + \beta\left[\boldsymbol{\nabla}\rho_0(\mathbf{r})\right]\cdot\left[\boldsymbol{\nabla}\rho_0(\mathbf{r})\right]\right] \delta_{\mathbf{r}_1,\mathbf{r}_2}\, \delta_{\mathbf{r}_1,\mathbf{r}'_1}\, \delta_{\mathbf{r}_2,\mathbf{r}'_2}$$

- Contribution to the single-particle potential $U_q(r)$

$$\begin{aligned} U_{\text{pair},q}(\mathbf{r}) \quad = \quad & \sum_{q'} \tilde{\rho}^*_{q'}(\mathbf{r})\, \tilde{\rho}_{q'}(\mathbf{r})\, B^{\tilde{\rho}\tilde{\rho}\rho}_{q'} \frac{\gamma_{q'}\, \rho_0^{\gamma_{q'}-1}(\mathbf{r})}{\rho_{\text{sat}}^{\gamma_{q'}}} \\ & -2\sum_{q'} C^{\tilde{\rho}\tilde{\rho}\nabla\rho\nabla\rho}_{q'} \left\{ \tilde{\rho}^*_{q'}(\mathbf{r})\, \tilde{\rho}_{q'}(\mathbf{r}) \left[\Delta\rho_0(\mathbf{r})\right] + \left[\boldsymbol{\nabla}\tilde{\rho}^*_{q'}(\mathbf{r})\, \tilde{\rho}_{q'}(\mathbf{r})\right]\cdot\left[\boldsymbol{\nabla}\rho_0(\mathbf{r})\right] \right\} \end{aligned}$$

- Fayans pairing energy density functional has an quadrilinear gradient term

$$E^{\text{Fy}}_{\text{pair}} = \int d^3r \sum_q \tilde{\rho}^*_q(\mathbf{r})\,\tilde{\rho}_q(\mathbf{r}) \left\{ A^{\tilde{\rho}\tilde{\rho}}_q + B^{\tilde{\rho}\tilde{\rho}\rho}_q \left[\frac{\rho_0(\mathbf{r})}{\rho_{\text{sat}}}\right]^{\gamma_q} + C^{\tilde{\rho}\tilde{\rho}\nabla\rho\nabla\rho}_q \left[\boldsymbol{\nabla}\rho_0(\mathbf{r})\right]\cdot\left[\boldsymbol{\nabla}\rho_0(\mathbf{r})\right] \right\}$$

which corresponds to a two-body pairing force of the form

$$v_{\text{pair}}(\mathbf{r}_1,\mathbf{r}_2,\mathbf{r}'_1,\mathbf{r}'_2) = \hat{\Pi}_{S=0}\, V_0 \left[1+\alpha\left(\frac{\rho_0(\mathbf{r})}{\rho_{\text{sat}}}\right)^{\gamma} + \beta\left[\boldsymbol{\nabla}\rho_0(\mathbf{r})\right]\cdot\left[\boldsymbol{\nabla}\rho_0(\mathbf{r})\right]\right] \delta_{\mathbf{r}_1,\mathbf{r}_2}\,\delta_{\mathbf{r}_1,\mathbf{r}'_1}\,\delta_{\mathbf{r}_2,\mathbf{r}'_2}$$

- Contribution to the single-particle potential $U_q(r)$

$$\begin{aligned} U_{\text{pair},q}(\mathbf{r}) &= \sum_{q'} \tilde{\rho}^*_{q'}(\mathbf{r})\,\tilde{\rho}_{q'}(\mathbf{r})\; B^{\tilde{\rho}\tilde{\rho}\rho}_{q'}\; \frac{\gamma_{q'}\,\rho_0^{\gamma_{q'}-1}(\mathbf{r})}{\rho_{\text{sat}}^{\gamma_{q'}}} \\ & \quad -2\sum_{q'} C^{\tilde{\rho}\tilde{\rho}\nabla\rho\nabla\rho}_{q'} \left\{\tilde{\rho}^*_{q'}(\mathbf{r})\,\tilde{\rho}_{q'}(\mathbf{r})\left[\Delta\rho_0(\mathbf{r})\right] + \left[\boldsymbol{\nabla}\tilde{\rho}^*_{q'}(\mathbf{r})\,\tilde{\rho}_{q'}(\mathbf{r})\right]\cdot\left[\boldsymbol{\nabla}\rho_0(\mathbf{r})\right]\right\} \end{aligned}$$

- $B^{\tilde{\rho}\tilde{\rho}\rho}_q$ and $C^{\tilde{\rho}\tilde{\rho}\nabla\rho\nabla\rho}_q$ can be chosen such that the contribution of the pairing EDF to the single-particle potential is the same and always repulsive.
- Because of the $\tilde{\rho}^*_{q'}(\mathbf{r})\,\tilde{\rho}_{q'}(\mathbf{r})$ factor, the contribution to $U_q(r)$ scales with the amount of pairing correlations.
- In odd nuclei, the (repulsive) contribution to $U_q(r)$ is smaller, such that the potential is slightly deeper, such that nucleons of both species are slightly more bound (on the order of 100 keV) and have shorter tails, which leads to smaller radii of less paired systems.
- As long as $B^{\tilde{\rho}\tilde{\rho}\rho}_q$ is finite, the above argument is still valid for $C^{\tilde{\rho}\tilde{\rho}\nabla\rho\nabla\rho}_q = 0$.

- We will first look into traditional "surface pairing" without gradient terms.

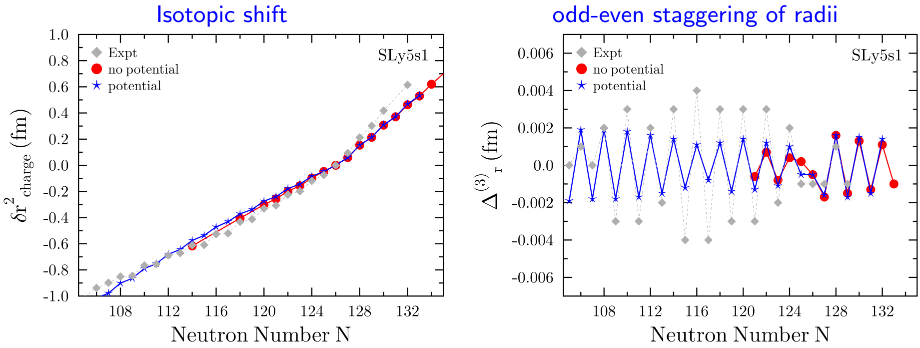


- "no potential": traditional neglect of the contribution to the potential $U(\mathbf{r})$ as in earlier papers
- "potential"

Blocking the 1qp state with experimental $K = J$ in odd systems

Isotope shift

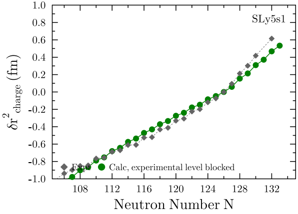


odd-even staggering of radii

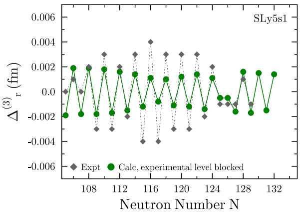


odd-even staggering of masses

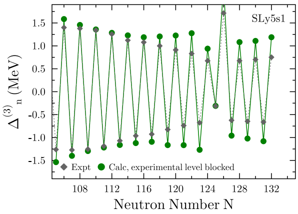

Blocking the 1qp state with experimental $K = J$ in odd systems

Isotope shift | odd-even staggering of radii | odd-even staggering of masses

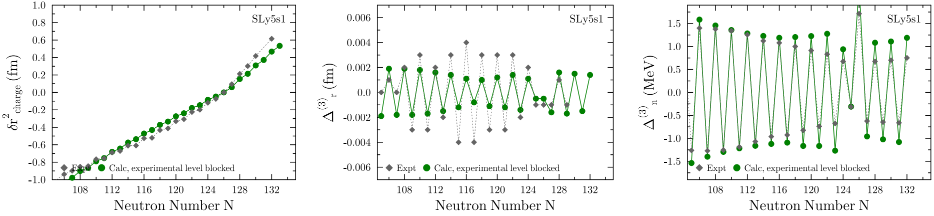


Blocking the lowest state in odd systems

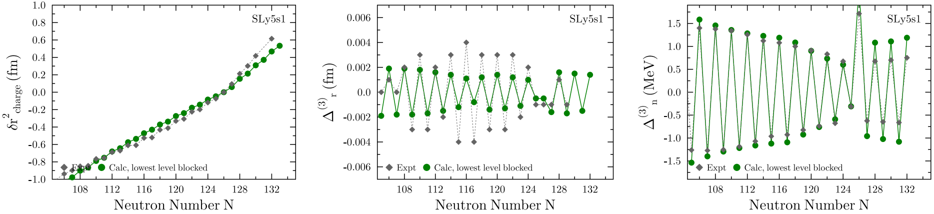


see Reinhard & Nazarewicz, PRC 95 (2017) 064328 for definition of the measures for staggering

Bender & Ryssens, unpublished

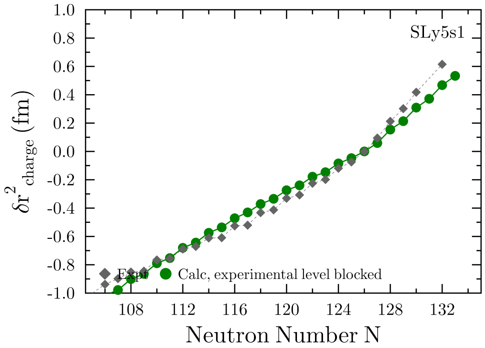


- Surface pairing EDF with strength of $-1250\,\text{MeV}\,\text{fm}^{-3}$
- Handling of the pairing EDF differs from other plots by the use of pure HFB (instead of HFB+LN) and considering the (in the past neglected) contribution of the pairing EDF to the single-particle Hamiltonian $\hat{h}$.

- The angle of the "kink" is reproduced

$$\epsilon_{\text{calc}} = \frac{\delta\langle r^2\rangle_{128,126}}{\delta\langle r^2\rangle_{126,124}} = 1.82$$

$$\epsilon_{\text{expt}} = 1.79$$

  but not the actual slopes, which are too small above *and* below $N = 126$.
- The slopes of calculated and experimental values change differently when going further away from $N = 126$
- The only information about Pb entering the fit of the SLy5SX are binding energy and charge radius of $^{208}$Pb.

Bender & Ryssens, unpublished

# Magnetic moments of Pb isotopes

- The state with experimental $J^\pi$ is blocked (which is not always the calculated ground state with SLy5s1)
- Symmetry-breaking self-consistency reduces magnetic moments compared to the Schmidt values, but by far not enough to match data.
- SLy5SX parameterizations were fitted with a constraint on stability against finite-size instabilities such that their "native" time-odd terms (spin-spin interactions etc) can be used without introducing convergence problems [Hellemans et al, PRC 88 (2013) 064323]. This does not mean that these terms have a realistic size, though.

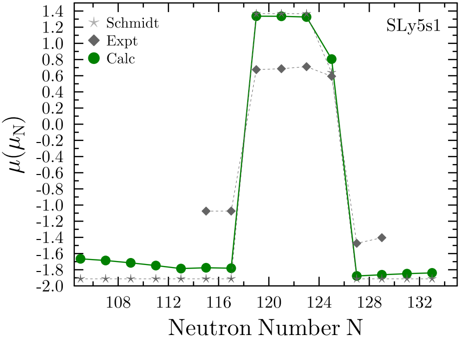


Bender & Ryssens, unpublished

Blocking the lowest 1qp state in odd systems

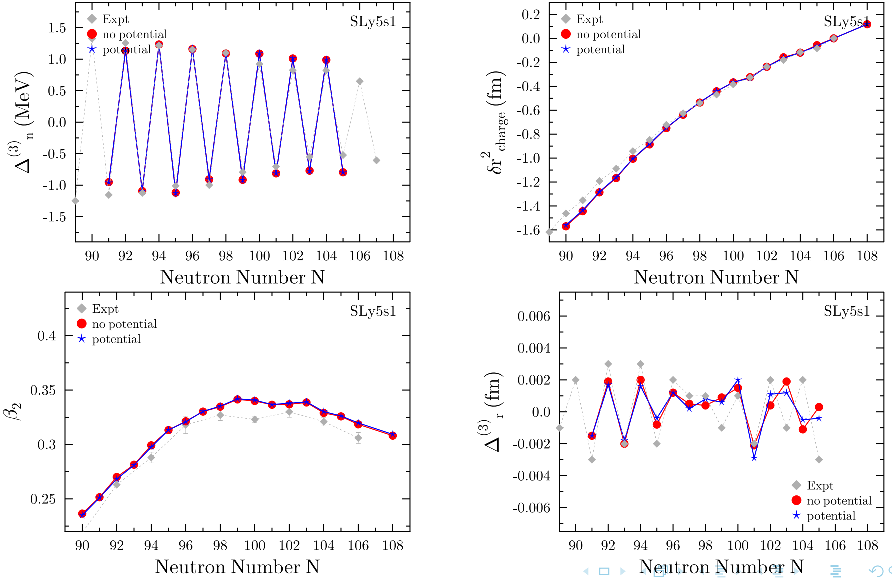

# Charge radii of Yb ($Z = 70$) isotopes – normal staggering

Blocking the 1qp state with experimental $K = J$ in odd systems

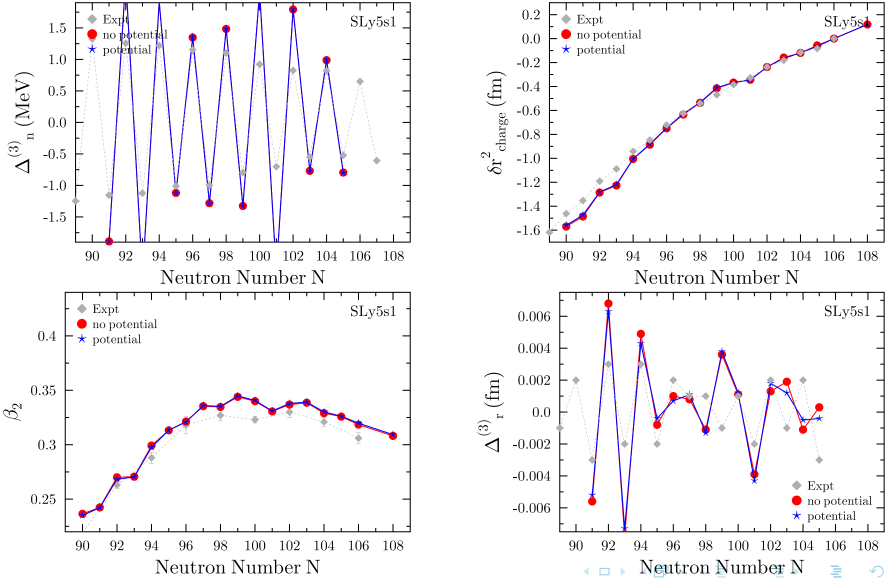

In a deformed odd system, the radius depends on

- the nodal structure of the blocked state
- the slope of blocked states in the Nilsson diagram

$\Rightarrow$ each configuration has a different deformation and radius!

Example: Low-lying band heads of $^{163}$Yb

| state | energy | rms_p | rms_n | beta_20 |
|---|---|---|---|---|
| 3.5- | -1310.012 | 5.1588 | 5.2279 | 0.2475 |
| 3.5+ | -1310.268 | 5.1760 | 5.2448 | 0.2915 |
| 1.5- | -1310.517 | 5.1635 | 5.2343 | 0.2703 |
| 2.5- | -1310.884 | 5.1595 | 5.2294 | 0.2576 |
| 2.5+ | -1311.341 | 5.1768 | 5.2460 | 0.2975 |
| 0.5- | -1311.542 | 5.1713 | 5.2409 | 0.2841 |
| 5.5- | -1311.632 | 5.1850 | 5.2546 | 0.3127 |
| 0.5+ | -1311.695 | 5.1684 | 5.2370 | 0.2782 |
| 1.5+ | -1311.741 | 5.1716 | 5.2407 | 0.2874 |
| 1.5- | -1311.838 | 5.1702 | 5.2396 | 0.2850 |
| 2.5- | -1311.872 | 5.1690 | 5.2377 | 0.2810 |

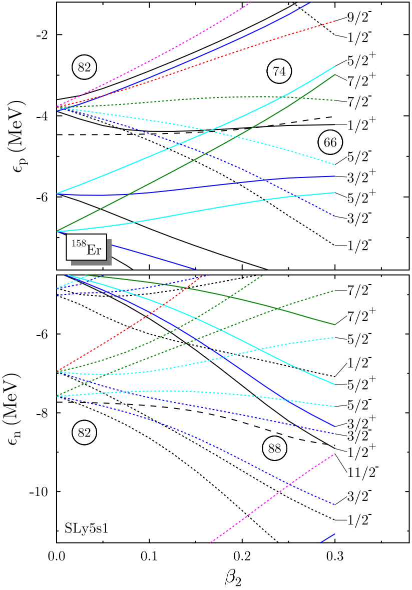

Blocking the lowest 1qp state in odd systems

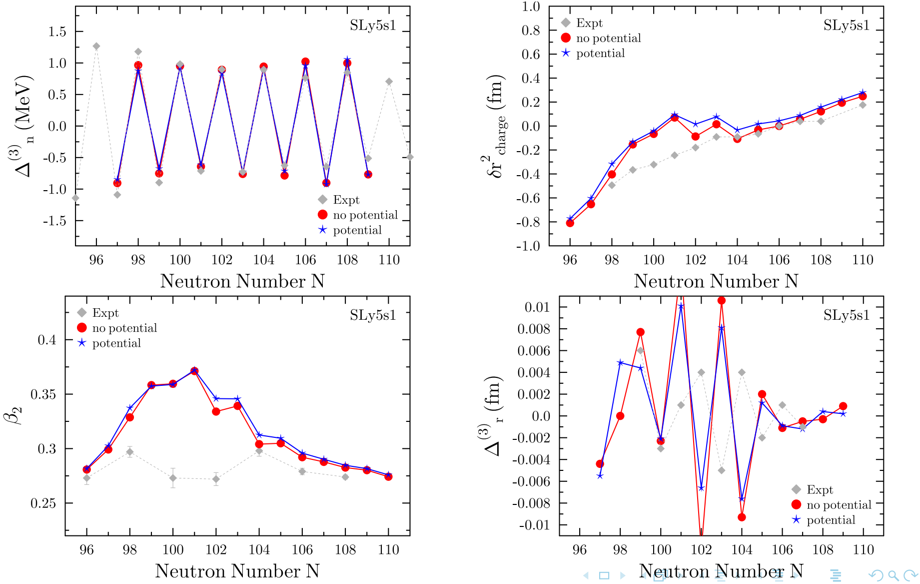

# Charge radii of Hf ($Z = 72$) isotopes – normal staggering

Blocking the 1qp state with experimental $K = J$ in odd systems

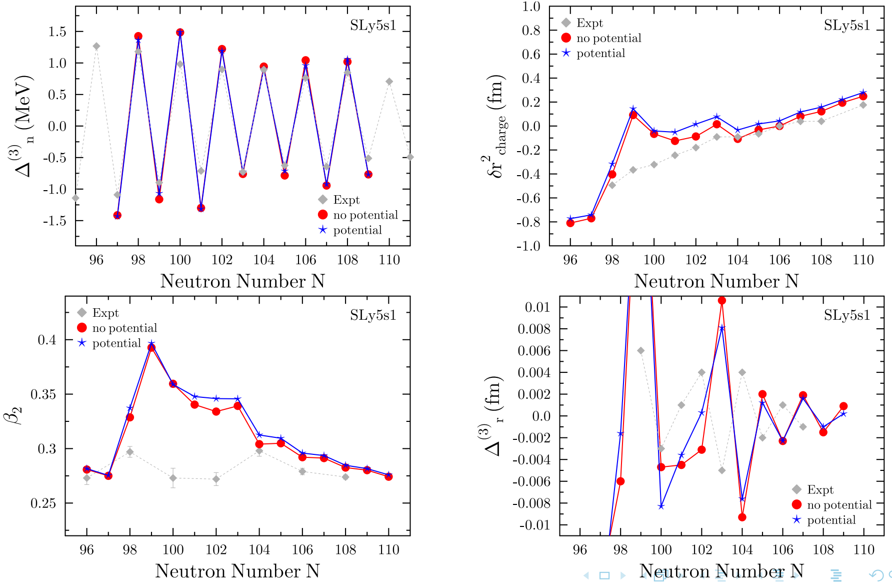

Blocking the lowest 1qp state in odd systems

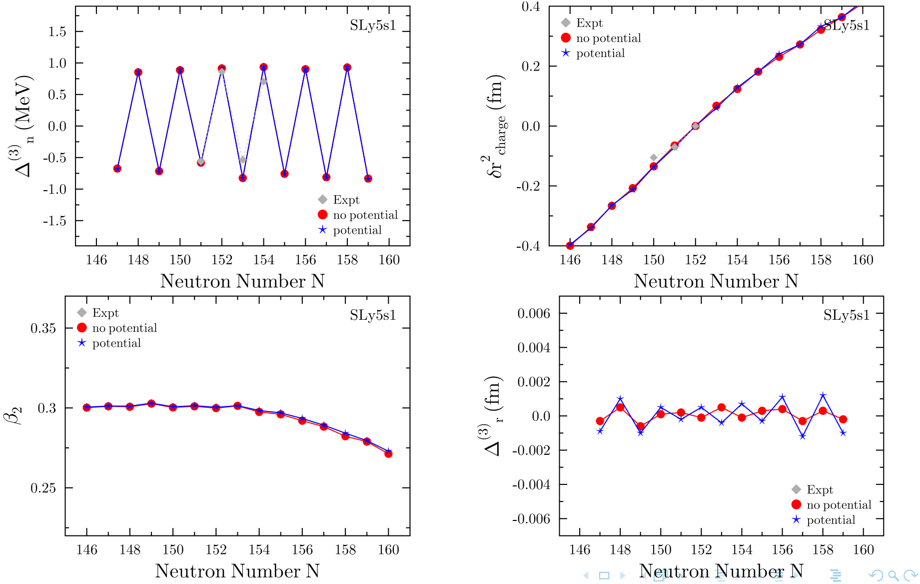

# Charge radii of No ($Z = 102$) isotopes – normal staggering

Blocking the 1qp state with experimental $K = J$ in odd systems

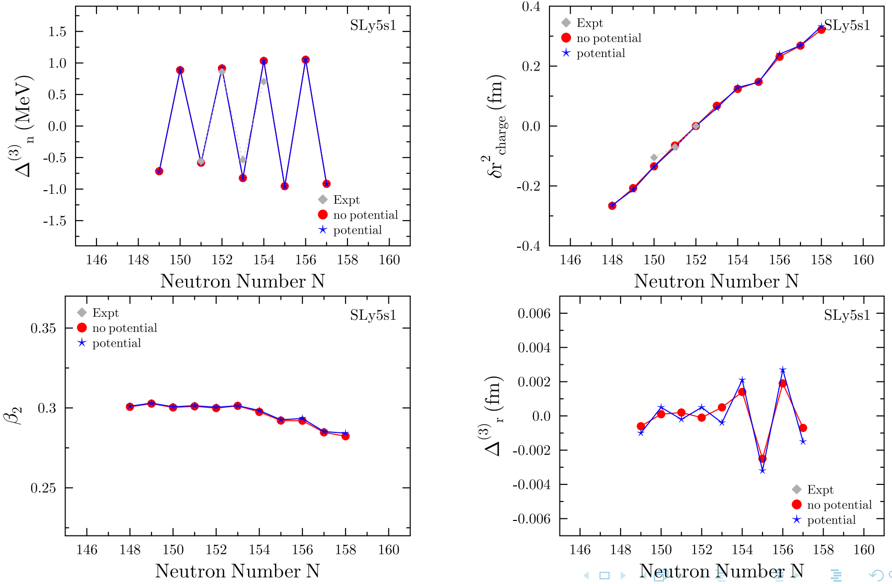

two mean-field calculations with SLy5s1 as above

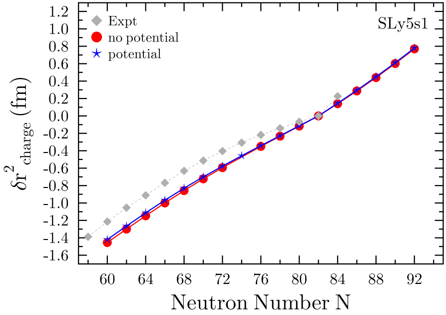


Bender & Ryssens, unpublished

Calculation with SLy4 "going beyond the mean field"

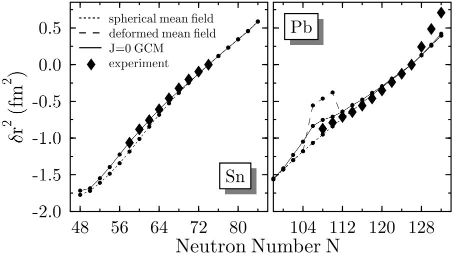


M. Bender, G. F. Bertsch and P.-H. Heenen, PRC 69 (2004) 034340

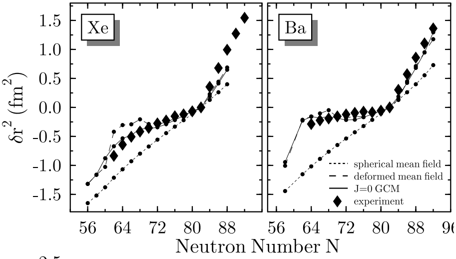


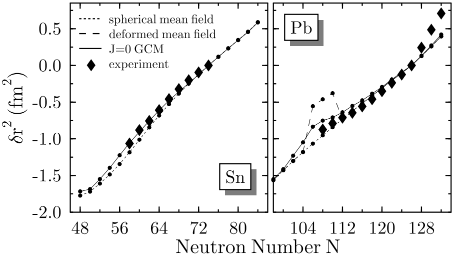


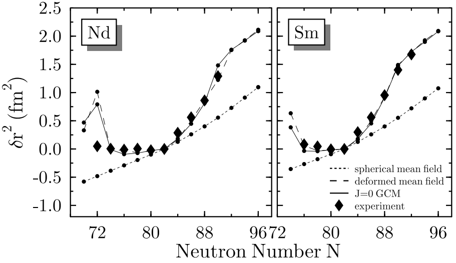


- Calculation with SLy4 comparing spherical mean field, deformed mean-field and symmetry-restored GCM
- For non-magic $Z$, the kink at closed shell $N$ might be because of disappearance of deformation (below) and/or onset of deformation (above).

M. Bender, G. F. Bertsch and P.-H. Heenen, PRC 69 (2004) 034340

# Take-away messages

- Most Skyrme EDFs found in the literature have a too large surface energy coefficient $a_{\mathrm{surf}}$.
- Fine-tuning the $a_{\mathrm{surf}}$ of the nuclear EDF brings a large improvement for many observables that are sensitive to deformation.
- Pairing EDF adjusted to reproduce kinematical moments of inertia of the SD band in the $A \approx 190$ region [Rigollet et al, PRC 59, 3120 (1999)] describes staggering of masses very well when the lowest state in the odd-mass system is chosen. Description of mass changes only marginally when taking the contribution of the pairing EDF to the potentials $U_q(\mathbf{r})$ into account.
- Systematic calculation of charge radii of spherical and well-deformed nuclei for several isotopic chains of heavy nuclei taking into account polarisation effects from symmetry-breaking.
- Qualitative difference between size and origin of the odd-even staggering of charge radii in spherical and deformed systems.
- Quality of radii and quality of staggering depend on quality for deformation.
- Rapid shape transitions can lead to inverted staggering of radii.

The work presented here would have been impossible without my collaborators

founding fathers

| | |
|---|---|
| Paul Bonche | SPhT, CEA Saclay |
| Hubert Flocard | CSNSM Orsay |
| Paul-Henri Heenen | Université Libre de Bruxelles |

formal aspects of the big picture

| | |
|---|---|
| Thomas Duguet | Irfu/CEA Saclay |
| Denis Lacroix | IPN Orsay |

design and implementation of code extensions

| | |
|---|---|
| Benoît Avez | CEN Bordeaux Gradignan |
| Benjamin Bally | formerly CEN Bordeaux Gradignan, now UNC Chapel Hill |
| Veerle Hellemans | Université Libre de Bruxelles |
| Jiangming Yao | Université Libre de Bruxelles |
| Wouter Ryssens | formerly UL Bruxelles, then IPN Lyon, now Yale |

development and benchmarking of new functionals

| | |
|---|---|
| Karim Bennaceur | IP2I Lyon |
| Dany Davesne | IP2I Lyon |
| Robin Jodon | IPN Lyon |
| Jacques Meyer | IP2I Lyon |
| Alessandro Pastore | formerly IPN Lyon, now University of York |
| Jeremy Sadoudi | Irfu/CEA Saclay first, then CEN Bordeaux Gradignan |

color code: active (past) member of the collaboration